

Diffusion of gases dissolved in peat pore water

R.S. Clymo¹ and M.M.R. Williams²

¹School of Biological and Chemical Sciences, Queen Mary University of London, E1 4NS, UK

²Applied Modelling and Computation Group, Department of Earth Science and Engineering, Imperial College of Science, Technology and Medicine, University of London, SW7 2BP, UK

SUMMARY

Diffusion is usually thought to be ineffective at transporting solutes over distances of several metres – the depth of many peat deposits. But this is to neglect the importance of time. We derive equations that show that in peat that has accumulated over millennia then diffusion alone can remove to the air about 95 % of the gases carbon dioxide and methane generated by microbial decay within the main peat mass. Gas concentration profiles in simulations of peat grown slice-by-slice over 10,000 years have a smooth convex profile with concentration increasing downwards, as they do in Nature.

KEY WORDS: analysis; anoxic; carbon dioxide; decay; diffusion; methane; peat growth

INTRODUCTION

Peatlands cover about 3 % of the Earth's land surface and contain nearly as much carbon as does the atmosphere (Clymo *et al.*, 1998). The surface layer, down to the depth to which the watertable sinks in a dry year, is the acrotelm (Ingram 1978). This depth is typically 5–60 cm below the surface. Within the acrotelm, with its subsidiary structural layers, the watertable moves down and up, and process zones move with the watertable too. Above the watertable aerobic processes dominate in the oxic conditions; a few cm below the watertable conditions become anoxic and anaerobic processes, particularly CH₄ production, dominate (Clymo & Pearce 1995). It is sometimes useful (Clymo & Bryant 2008) to subdivide the acrotelm into the predominantly oxic 5–20 cm thick layer at the top – the 'oxytelm' – and the usually anoxic (but periodically oxic) perhaps 30-cm thick 'mesotelm' below it. The boundary between these two may be at about the mean watertable (or the peat surface in pools).

Gases such as O₂, CH₄, CO₂, H₂ and N₂ move through the acrotelm by four processes: (1) diffusion; (2) ebullition (as bubbles); (3) through gas spaces in plant roots and stems, by diffusion and pressure driven mass flow (the plant bypass or shunt mechanism); (4) for CH₄, by oxidation to CO₂. Several computer simulations have been made (for example Walter *et al.* 1996, Grant & Roulet 2002, Zhuang *et al.* 2007, Wania *et al.* 2010) of the production and movement of gases by these four processes in the acrotelm. These models have up to

30 parameters. Many are fixed at reasonable values; others may be optimised by comparison with measured effluxes.

Below the oxytelm/mesotelm is the catotelm which is permanently anoxic. In a 7 m deep peat deposit the catotelm is more than ten times the depth of the acrotelm. Within it the concentration of CH₄ and CO₂ increases with depth (for example, among others, Clymo & Pearce 1995, Romanowicz *et al.* 1995, Clymo & Bryant 2008) – consistent with continued decay, though at a much lower rate than in the acrotelm. Two of the acrotelm models show that about 5 % of the efflux of CH₄ through the acrotelm may be by diffusion. For the catotelm, however, of the four processes which move gases in the acrotelm, only diffusion is plausible (we ignore oxidation of CH₄ because, as will become clear, CO₂ and CH₄ have nearly the same diffusion coefficient). Diffusion in the catotelm has been modelled by Romanowicz *et al.* (1995) and by Clymo & Bryant (2008). The acrotelm models above seem to make no provision for supply of gases from the catotelm below, nor is it clear what boundary condition is used at the base of the oxytelm/mesotelm. The lower boundary condition of the Romanowicz *et al.* model is the depth at which CH₄ concentration becomes saturating, and the model includes mass flow too.

In none of these models can one understand the rôle of diffusion by itself. In this article we now derive equations describing one-dimensional diffusion of a gas through a water-saturated medium. We show how the gas concentration depends on the position and type of its source, and on the passage of time.

METHODS

Derivation of the diffusion equations

We consider the diffusion of gas molecules in an unstirred (unmoving), isotropic, isothermal water-saturated layer of thickness X (Figure 1). At the top of the layer at $x = 0$ molecules escape to the air and the concentration in the topmost infinitely thin layer of the peat is taken to be zero. This is not strictly true because, physically, a more accurate boundary condition would be that there are no molecules returning to the surface. However, a zero concentration condition is a very close approximation to this and simplifies the analysis considerably. At the base of the layer, $x = X$, the

underlying solid is impermeable. Physically this implies that there is no net flow of molecules across the plane, which acts as a perfect mirror would for light, and hence the gradient of the concentration is zero. We suppose that the effective diffusion coefficient, D , is reduced by the presence of peat solids, from its value in pure water, D_w .

We consider two problems. The first (P1) follows the fate of a gas initially in a thin layer in a peat column entirely without the gas everywhere else. The second problem (P2) follows the more immediately realistic situation with a peat initially free of the gas, but thereafter gas is added to a thin layer continuously, as it might be with continuing decay of the peat.

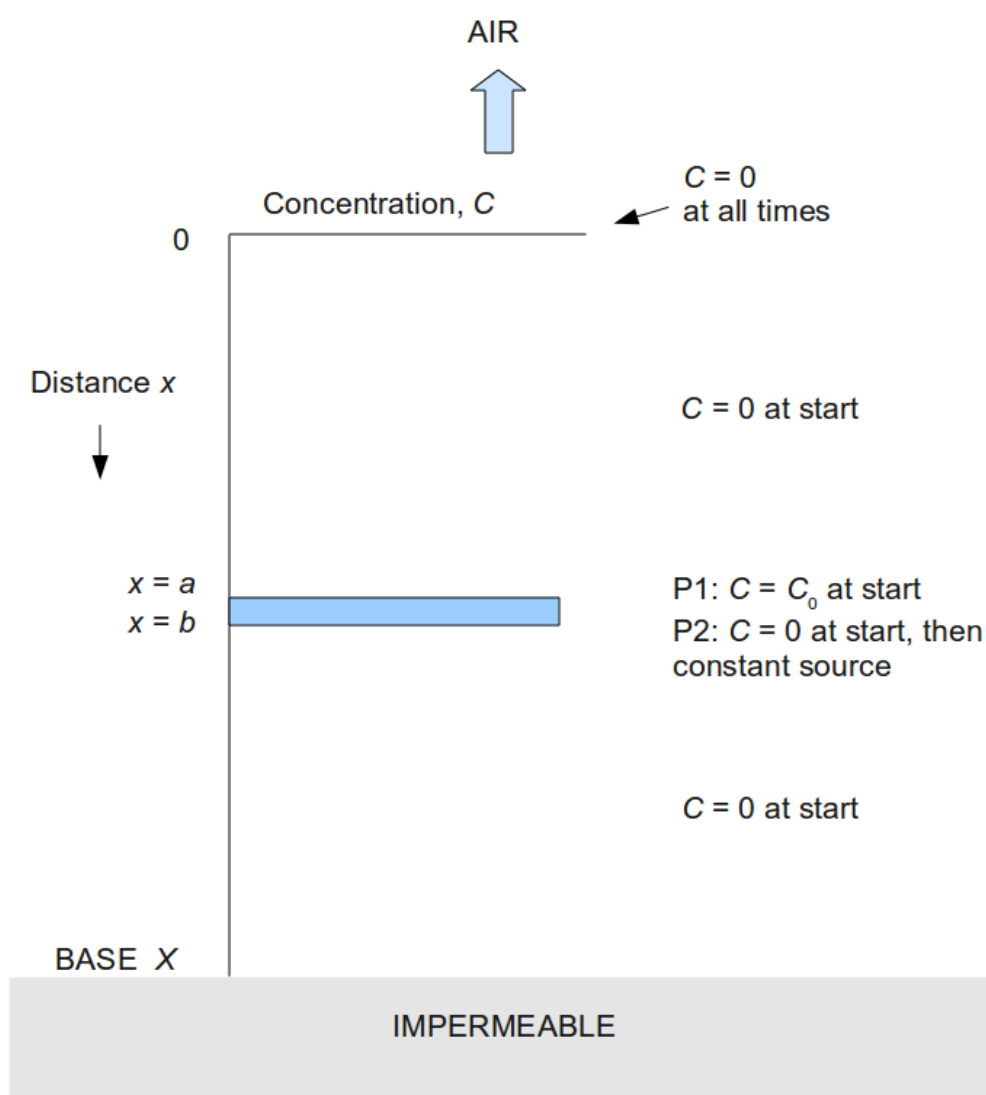


Figure 1. The diffusion problems: concentration as a function of depth. At the surface at $x = 0$ the concentration is supposed zero at all times: $C = 0$. Problem 1 (P1) is 'one-shot' with concentration C_0 at the start in the layer $a < x < b$ and zero everywhere else; the amount of gas in the system decreases continuously as gas effluxes to the air. Problem 2 (P2) has initial concentration zero everywhere, then constant rate of addition of $1.0 \text{ unit of mass cm}^{-3} \text{ yr}^{-1}$ in the layer $a < x < b$; the amount of gas in the system increases continuously (towards an asymptote). In both problems gas molecules are redistributed by diffusion.

Problem 1: (P1, one-shot) initial concentration zero except in the slab between $x = a$ and $x = b$

The initial condition at $t = 0$ is zero concentration everywhere except for a uniform distribution of gas in a layer $a < x < b$, where $0 < a < b < X$. Assuming diffusion theory is valid we may model the problem mathematically as follows with $C(x,t)$ the concentration of gas molecules at x at time t and with D the diffusion coefficient.

$$\frac{\partial C(x,t)}{\partial t} = D \frac{\partial^2 C(x,t)}{\partial x^2} \quad (1)$$

Boundary conditions are

$$C(0,t) = 0 \quad (2)$$

and

$$\text{current} = -D \frac{\partial C(x,t)}{\partial x} \Big|_{x=X} = 0 \quad (3)$$

The initial condition is

$$\begin{aligned} C(x,0) &= C_0; & a < x < b \\ C(x,0) &= 0; & 0 < x < a, \quad b < x < X \end{aligned} \quad (4)$$

We solve Equation (1) by writing

$$C(x,t) = \sum_{n=0}^{\infty} C_n(t) \sin(\alpha_n x) \quad (5)$$

where

$$\alpha_n = \frac{(2n+1)\pi}{2X} \quad (6)$$

Equation (5) automatically satisfies the boundary conditions (2) and (3). For simplicity we define

$$E_n(x) = \sin(\alpha_n x) \quad (7)$$

which obeys the orthogonality condition

$$\int_0^X E_n(x) E_m(x) dx = \frac{X}{2} \delta_{nm} \quad (8)$$

Inserting (5) into (1), multiplying by $E_m(x)$, integrating over $x(0,X)$ and using (8) leads to

$$\frac{dC_m(t)}{dt} = -D\alpha_m^2 C_m(t) \quad (9)$$

Equation (9) can be solved to give

$$C_m(t) = C_m(0) \exp(-D\alpha_m^2 t) \quad (10)$$

To obtain $C_m(0)$, we note from (5) that

$$C(x,0) = \sum_0^{\infty} C_n(0) \sin(\alpha_n x) \quad (11)$$

Using (4), multiplying (11) by $E_m(x)$ and integrating over $x(0,X)$, we find

$$\int_0^x E_m(x)C(x,0)dx = C_m(0) \frac{X}{2} \quad (12)$$

whence

$$C_m(0) = \frac{2C_0}{X} \int_a^b dx E_m(x) = \frac{8C_0}{(2m+1)\pi} \sin\left(\frac{\alpha_m(a+b)}{2}\right) \sin\left(\frac{\alpha_m(b-a)}{2}\right) \quad (13)$$

Thus inserting Equation (13) into (10), and (10) into (5), we have

$$C(x,t) = \frac{8C_0}{\pi} \sum_{n=0}^{\infty} \frac{1}{(2n+1)} \exp(-D\alpha_n^2 t) \sin\left(\frac{\alpha_n(a+b)}{2}\right) \sin\left(\frac{\alpha_n(b-a)}{2}\right) \sin(\alpha_n x) \quad (14)$$

Problem 2: (P2, constant source) initial concentration zero and a constant source in the layer between $x=a$ and $x=b$

The second problem arises if, instead of the concentration in the region (a, b) being instant at $t=0$ and then switching off, it remains as a constantly emitting source for all time $t > 0$. The solution to this problem can be obtained directly from Problem 1 if we regard the initial condition (4) to be replaced by a constantly emitting source S_0 , with units of molecules per unit area of the source layer per unit time. It is then clear that

$$C_S(x,t) = \int_0^t dt_0 C(x,t_0) \quad (15)$$

where S is the solution we seek and in $C(x,t)$ we replace C_0 by S_0 . From (14) we find

$$C_S(x,t) = \frac{8S_0}{\pi} \sum_{n=0}^{\infty} \frac{1}{(2n+1)D\alpha_n^2} [1 - \exp(-D\alpha_n^2 t)] \sin\left(\frac{\alpha_n(a+b)}{2}\right) \sin\left(\frac{\alpha_n(b-a)}{2}\right) \sin(\alpha_n x) \quad (16)$$

We note that as $t \rightarrow \infty$, the concentration $C_S(x,\infty)$ is equal to

$$C_S(x,\infty) = \frac{8S_0}{\pi} \sum_{n=0}^{\infty} \frac{1}{(2n+1)D\alpha_n^2} \sin\left(\frac{\alpha_n(a+b)}{2}\right) \sin\left(\frac{\alpha_n(b-a)}{2}\right) \sin(\alpha_n x) \quad (17)$$

This can be simplified to

$$\begin{aligned} C_S(x,\infty) &= \frac{S_0}{D}(b-a)x && ; 0 \leq x \leq a \\ C_S(x,\infty) &= \frac{S_0}{2D}(2xb - x^2 - a^2) && ; a \leq x \leq b \\ C_S(x,\infty) &= \frac{S_0}{2D}(b^2 - a^2) && ; b \leq x \leq X \end{aligned} \quad (18)$$

These solutions were programmed in C++.

In P2, for long diffusion times and large distances from the source, as the number of terms in Equation (17) increases there appear series of alternating increasingly large positive then large negative values. These are followed by series of alternating but decreasing terms (ringing). The summation must be continued, sometimes for more than 100 terms, until a sequence of 20 successively smaller absolute differences between adjacent (successive) terms. A measure of accuracy of the summation was obtained by comparing the solution of (17) with the analytically summed solution (18). Accuracy to 5 significant digits was established.

What value is suitable for the diffusion coefficient (D)?

There are several reports of the diffusion coefficient of gases in peat, but all deal with the acrotelm, in which the water content changes (and so does the pore space). We therefore consider measurements in a saturated immobile medium in closely controlled conditions. Jähne *et al.* (1987) made careful measurements at controlled temperature of diffusion coefficients (D_G) in 0.5 % agarose gel (so that mass movements of water were minimised, as they are in many, perhaps most, deep peats). They gave special attention to reducing several biases. They then inferred the diffusion coefficient in pure water (D_W) from D_G . While the values of D_W for the noble gases followed Graham's law closely, being related to $\sqrt{(\text{molecular mass})}$, those for CH_4 and CO_2 were 40 % and 73 % respectively of the Graham's law predictions. Further, the values of D_W for CH_4 and CO_2 were identical at 35 °C, and only 5 % different at 5 °C. Jähne *et al.* attribute these phenomena to the lack of a permanent dipole momentum in both gases, thus minimising interactions with the water molecules. For the temperature (T_c) range 5 to 35 °C the results for CH_4 and CO_2 are $D_W / \text{cm}^2 \text{ s}^{-1} = a \exp [(-2282 \times (1 / (273 + b T_c)) - 3.22)]$ where the constants a and b establish dimensional accuracy: $a = 1.0 \text{ cm}^2 \text{ s}^{-1}$; $b = 1.0 \text{ }^\circ\text{C}^{-1}$. This value of D_W must be reduced to allow for the peat solids. For our purposes we need D for a proportion of solid at least ten-fold greater than the 0.5 % of agarose solid mass (P_S) covered by Jähne *et al.* (1987). For dissolved solids it was shown by Slade *et al.* (1966) that, independent of the nature of the solute, the reduction factor $F = D / D_W$ for agar gels in the P_S range 0.01 to 0.04 then $F = 1 / (1 + 2.4 P_S)$. The agar seemed to behave as a simple mechanical obstruction with effects directly proportional to its mass. The graph lines were straight over this range, so a small extrapolation seems likely to be acceptable. A suitable value for $D = F D_W$ at 5 °C

and for P_S (for peat, this is the dry bulk density) 0.05 g cm^{-3} , D is $0.88\text{e-}5 \text{ cm}^2 \text{ s}^{-1}$ which, in more appropriate time units, is $278 \text{ cm}^2 \text{ yr}^{-1}$. This value was used in the illustrative Figures in the rest of this article. It is likely that at least some of the peat solids, being larger than gel solids, may require a further reduction for tortuosity, but we ignore that for the illustrations here.

RESULTS

In the examples which follow the source layer was 2 cm thick, spanning 29 yr, and the peat depth was 700 cm. Source layers 30 cm from the top, midway, and 30 cm from the base are illustrated. These are arbitrary choices.

The 'one-shot' (P1) model

Figure 2 illustrates the development of concentration profiles where the initial concentration in the source layer is known, and the molecules in the source gradually redistribute themselves. The concentration (abscissa) is scaled logarithmically to allow detail to be seen.

The centre graph, with the source at mid-depth shows, as one expects, that for the first 10 yr the concentration profiles are near symmetrical about the source layer. By that time the concentration in the source layer is only 1 % of the initial value, and concentrations a hundred times smaller are found 150 cm above and below the source layer. After 100 yr the profile has become asymmetric because gases cannot escape through the base but can into the air above. This trend continues with a further 3- to 10-fold reduction in concentration by 1000 yr, by which time only 20 % of the gas remains in the peat, while the rest has escaped to the air (Figure 4). Sources near the top or base of the peat show modifications of these patterns affected by the ease or difficulty of gas escaping to the air.

Some effects are not so obvious. For example, at 200 cm deep with the source at mid-depth the concentration increases between 10 and 100 yr, but then decreases between 100 and 1000 yr as the initial stock of molecules is spread ever further and increasingly is lost to the air. More generally the concentration profiles at different times cross one another.

In the left graph, where the source layer is near the surface, asymmetry is clear after only 10 years, resulting from loss to air alone. The shorter path to air also results in less than 2 % of gas remaining in the peat after 1000 yr (Figure 4). The reverse effect is seen in the rightmost graph where after 1000 yr about a third of the gas is still in the peat.

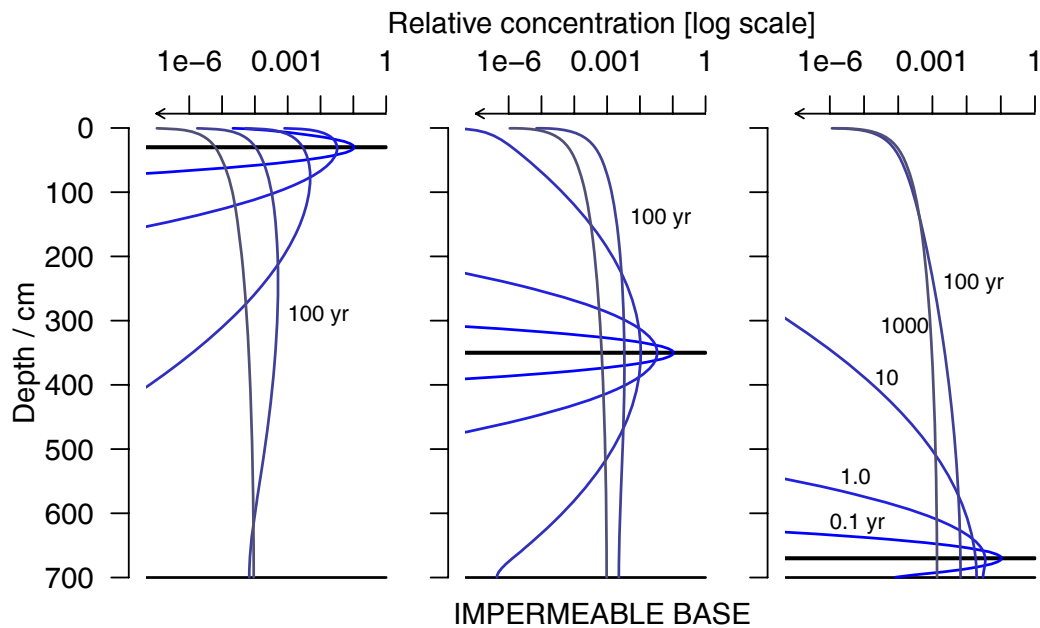


Figure 2. For Problem 1 (P1: 'one-shot') concentration profiles according to Equation (14) after six times (0, 0.1, 1, 10, 100, and 1000 yr) for three positions of a 2-cm thick source layer $a < x < b$: 30 cm from the top, mid-depth, and 30 cm from the base. The initial concentration in the source layer is 1.0 unit of mass cm^{-3} ; the diffusion coefficient is $278 \text{ cm}^2 \text{ yr}^{-1}$ – similar to that of carbon dioxide and of methane in water at about 5°C and with 5 % solid matter in the peat. The concentration is relative to the source being 1.0 unit of mass cm^{-3} (at the start), and is scaled logarithmically. In the left hand graph the concentration after 1000 yr is everywhere less than 1.0×10^{-4} units. Scales are the same for all three graphs and the same as those in Figure 3.

The constant source (P2) model

This model is closer to the real conditions in peat where decay continues, albeit very slowly. Figure 3 illustrates the development of concentration profiles where the initial concentration was zero everywhere but the source layer then generates gas at a constant rate. In contrast to the P1 model, the concentration profiles at different times (Figure 3) can never cross one another, and there is an asymptotic limit at infinite time (Equation (18)). For a source at the bottom of this 700 cm deep peat profile the asymptotic concentration limit is at 4.8 units (relative to the yearly rate of addition of 1 unit of gas mass $\text{cm}^{-3} \text{ yr}^{-1}$).

In the centre graph (Figure 3), where the source is midway down the peat, the log-scaled profiles are shaped like a symmetrical Bishop's mitre for the first 10 yr at least. (If the abscissa is untransformed, as in Figure 5, the convex shapes become concave, rising to a cusp at the source layer.)

The profile after 1 yr (when the same amount of gas has been supplied to P1 and P2) may be contrasted with the similar one in Figure 2. The difference results because in Figure 3 concentration starts at zero and addition is continuous, while in Figure 2 concentration began at 1.0 but then declined as no more gas was added.

Asymmetry develops (Figure 3) between 10 and 100 yr, as in the P1 model, but because gas is being added continuously at a rate of 1.0 unit of mass $\text{cm}^{-3} \text{ yr}^{-1}$ the concentrations eventually rise above 1.0. But the proportion of all gas added in the P2 model is, after the first year, always greater than at the same time in the P1 model. Figure 3 shows that for the middle source after 1000 yr about half remains (cf. 20 % in Figure 2) – but note that after 1000 yr in the P2 model 1000 times as much gas has been added as in the P1 model at the same time. In the bottom source, after 1000 yr, $2/3$ remains (compared with $1/3$ in the P1 model). Independent of where the source layer is, the concentration profile after 1000 yr is close to that at infinite time.

Figure 5 shows the data of Figure 3 replotted on linear axes – less detailed than the log transformed version but directly related to concentrations in the field. The curves all consist of two concave sections rising to a cusp at the source, and tending eventually (Equation (18)) to two straight lines; the lower vertical, the upper hinged at the source and pointing towards zero at the top. These are for a single thin (2 cm) layer, and do not resemble the smooth convex profiles of concentration recorded (e.g., by Clymo & Bryant 2008) for systems consisting of piles of layers accumulated steadily over millennia.

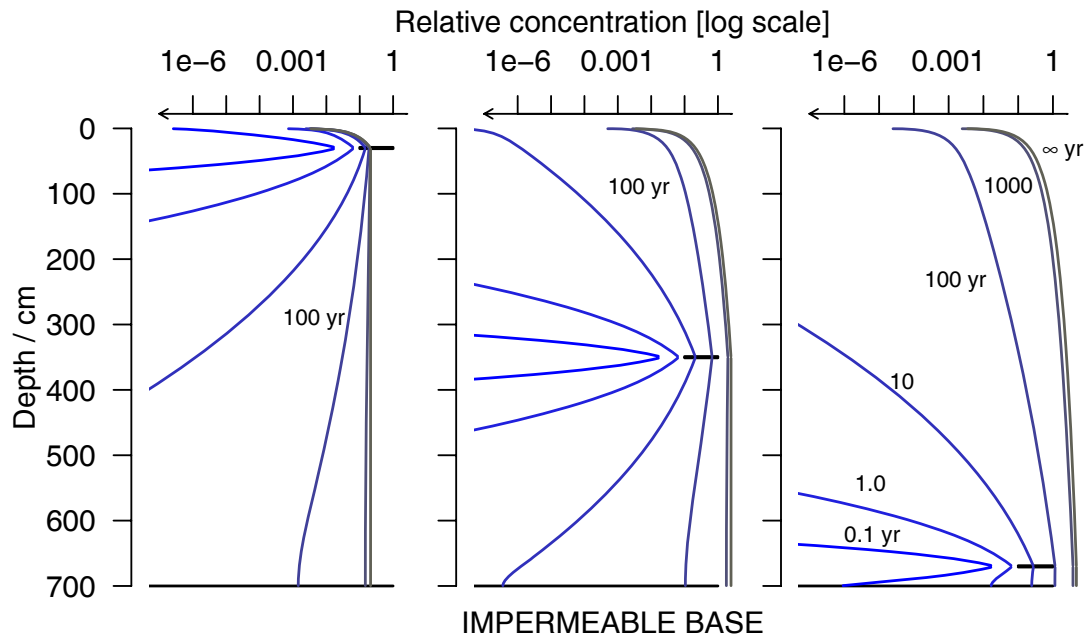


Figure 3. For Problem 2 (P2: constant source) concentration profiles according to Equation (17) after six times (0.1, 1, 10, 100, 1000 yr, and at infinite time) for three positions of the 2-cm thick source layer: 30 cm from the top, mid-depth, and 30 cm from the base. The rate of addition is 1.0 unit of mass $\text{cm}^{-3} \text{yr}^{-1}$; the diffusion coefficient is $278 \text{ cm}^2 \text{yr}^{-1}$ – similar to that of carbon dioxide and of methane in water at about 5°C and with 5 % solid matter in the peat. The concentration is relative to the source being 1.0 unit of mass cm^{-3} , and is scaled logarithmically. Initial concentration is zero at all depths so does not show on the log scale which starts at $1.0\text{e-}7$. The open horizontal bar shows the source layer; the right end of the bar is at value 1.0 on the abscissa in all three graphs. Scales are the same for all three graphs and the same as those in Figure 2.

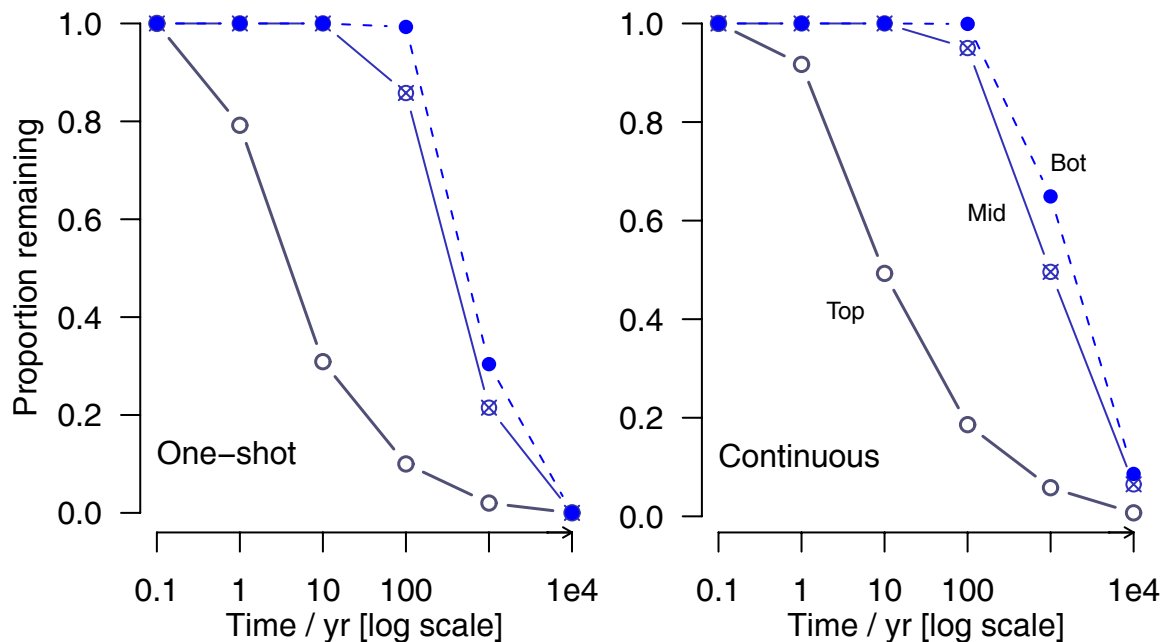


Figure 4. Proportion of the gas that has been added still in peat after six times (0.1, 1, 10, 100, 1000, 10 000 yr) for addition at the top (29 to 31 cm, empty circles), mid way (349 to 351 cm, crossed squares), and at the bottom (669 to 671 cm, filled circles). Left: for the 'one-shot' (P1) model in which the total gas added is 1.0 unit of mass cm^{-3} . Right: for the continuous addition (P2) model in which the total gas added is t units of mass cm^{-3} (t is the number of years elapsed from the start at $t = 0$).

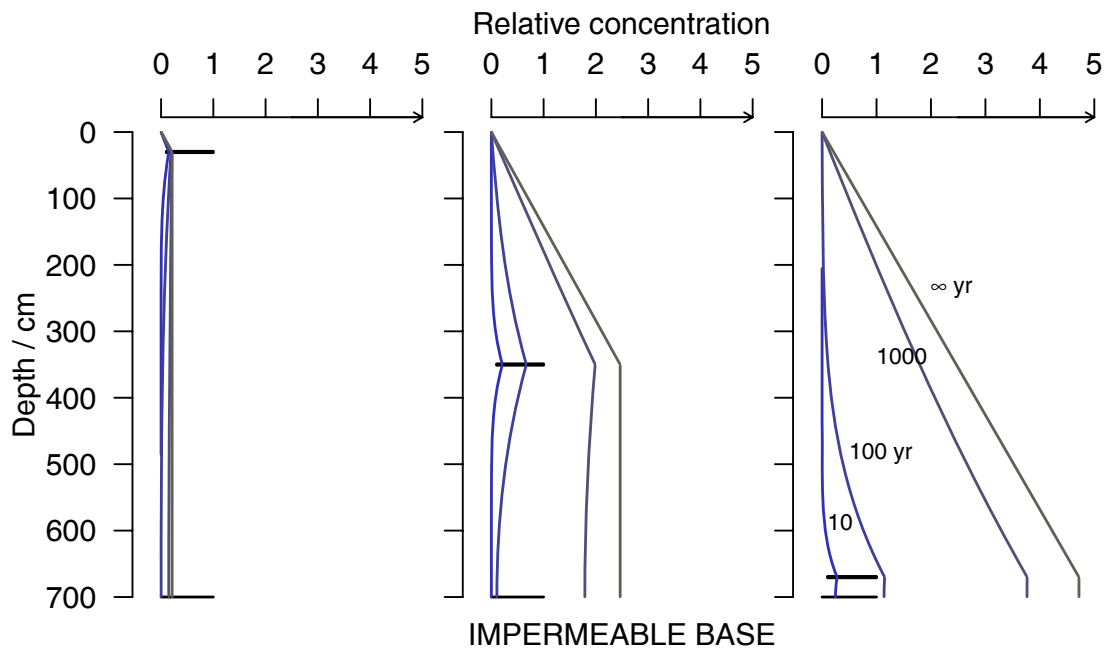


Figure 5. Same data as in Figure 3, but with relative concentration on a linear scale and for 10, 100, 1000 yr and infinite time only. The concentration is relative to the source being 1.0 unit of mass $\text{cm}^{-3} \text{yr}^{-1}$. The leftmost graph shows why the earlier Figures used a log scale. The middle and right graphs show that at infinite time the profile is close to two straight lines; the lower part vertical, and the upper hinged at the source depth to point to zero at the surface.

DISCUSSION

Fifty years ago the only way to understand a problem was by exact (mathematical) analysis of simplified – often over-simplified – situations. From the equations, understanding of the process emerged. Computer-power is now so great that it allows simulations of numerous simultaneous processes in heterogeneous environments, a common objective being to reproduce as exactly as possible the results observable in Nature. Such work is valuable, but it is often so complex that it gives little understanding of the individual processes. There is still a place, therefore, for the analysis of simplified situations, and this has been our purpose here.

Perhaps the most interesting finding is that from the P2 continuous source solution we see (Figure 3) that after 1000 yr the concentration profiles are close to the Equation (18) asymptote at infinite time. The oldest layer (right of Figure 3) has higher concentrations than any younger layer, so gases from the older layers dominate the overall profile.

One may ask: ‘What shape of profile results if these analyses for single thin layers are applied to a whole peat deposit as it accumulates over millennia?’ A computer simulation model was written in C++ for this purpose. Thin layers of peat were (notionally) added one after the other. At each addition a mass of gas was added to each of the layers accumulated so far. Then, for each layer in

turn its contained gas was redistributed using the P1 (‘one-shot’) model. This is realistic because molecular diffusion is a random process and at low dissolved gas concentrations such as we have here each dissolved gas molecule behaves almost independently of all others (though the summed effects are concentration dependent, as in Fick’s Law). The redistributions were made into stores parallel to the main ones, without altering the existing main stores that had not yet undergone redistribution. When all the layers had been potentially redistributed then the parallel stores overwrote the main ones, and the cycle began again, adding the next layer to the top. Of course simplification carries with it a degree of unreality. The top of our model is supposed to be the air though in a real peat deposit it is the base of the mesotelm, which is itself a major site of anoxic decay (Belyea 1996) and CH_4 production.

Four models of the rate of addition were tried (Figure 6). In ‘Z’ the rate of addition was constant at all depths and times. As the more labile components of peat decay, those that remain are more refractory. The ‘L’ model supposes that, as time passes, the rate of addition for any given layer decreases linearly with age from 1.0 at age zero towards 0.1 at the basal age (10 000 yr in the example). In the ‘Q’ model the decrease follows a negative exponential (Figure 6) towards the same total addition of mass of gas after 10 000 yr as there is in the linear model.

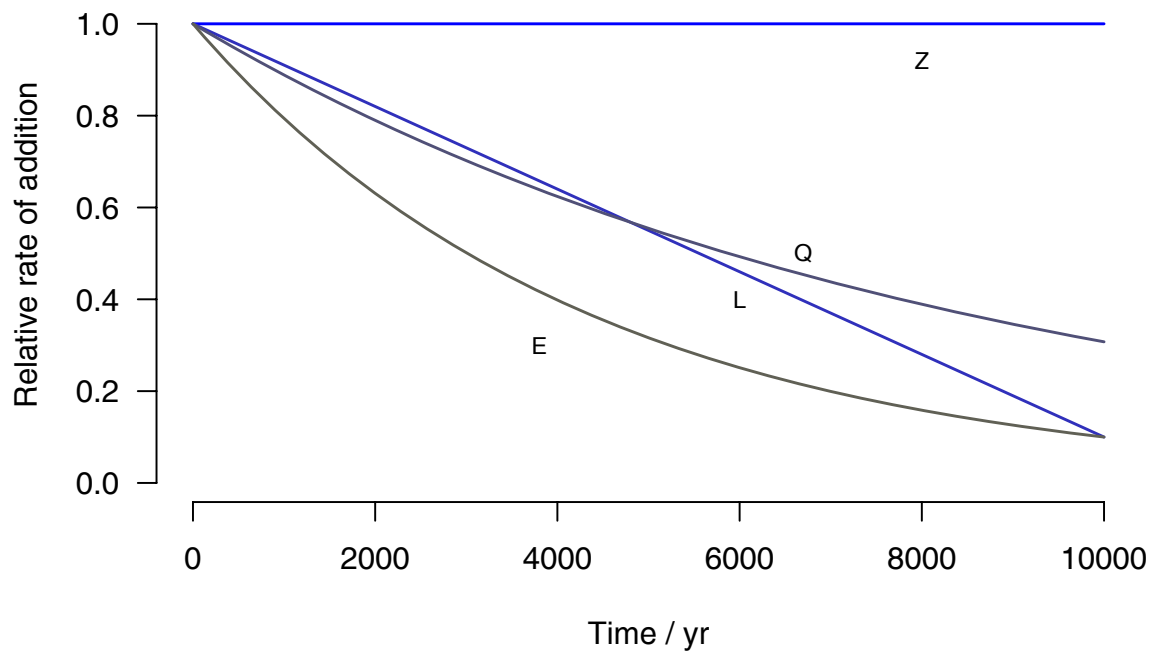


Figure 6. Four models for change in the rate of addition of gas mass with time. 'Z' = no (zero) change = constant rate of addition; 'L' = linear decline with depth and time from 1.0 to 0.1 at the end; 'Q' = negative exponential decline that, by the end, has added the same gas mass as the 'L' model; 'E' = negative exponential decline that, by the end, has reached the same value (0.1) as the 'L' model.

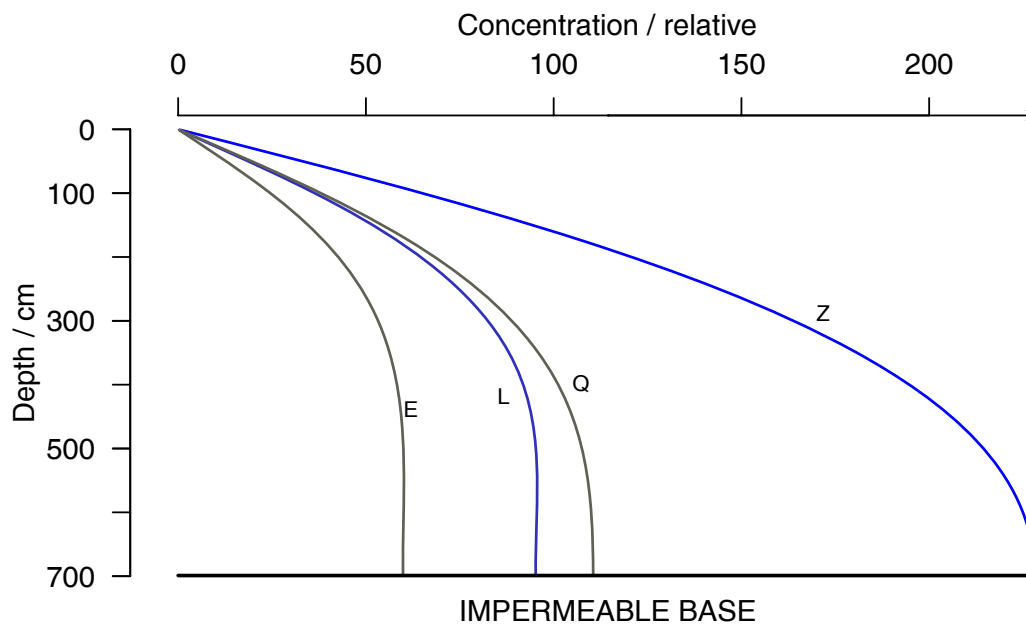


Figure 7. Peat grown (2 cm thick) layer by layer for 10 000 yr to a depth of 700 cm. After each new layer was added a new mass of gas was generated in every layer and added to that already present in the layer. Then a copy of the gas in each layer was allowed to diffuse following the P1 ('one-shot') equation and stored provisionally (to avoid altering the mass of gas in other layers before redistribution). Finally the provisional gas mass distributions were substituted for the existing gas mass in each layer. The results depend to a small extent on the time interval consequent on the choice of depth and time of accumulation. Seven such times were evaluated and the mean concentrations in each extrapolated to zero time. This gave a factor to apply to the results for a finite time to extrapolate them to a zero time interval. The four models 'E', 'L', 'Q' and 'Z' are for different changes in the rate of addition of gas mass with time (see Figure 6). The convex profiles of concentration resemble those observed in deep peat for CH₄ and CO₂ (for example, Clymo & Bryant 2008).

In the last 'E' model the decrease is again negative exponential but, as in the linear model, moving at 10 000 yr to 0.1 of the original rate.

Figure 7 shows the concentration profiles for a 700 cm deep peat grown in 2 cm layers (each spanning 29 yr) over 10 000 yr. At the right, the rate of addition was constant ('Z') at all depths and ages. All profiles are smooth and convex, just as measured ones are (e.g., Romanowicz *et al.* 1995, Clymo & Pearce 1996, Clymo & Bryant 2008).

The total mass of gas added in the linear decrease 'L' model was 70 % of that added in the 'Z' model, but the concentrations left in the peat are less than half those with the unchanging 'Z' rate of addition. The relatively high rates of loss to the air from young layers are not compensated by continuing high generation rates in the lower peat (as in the 'Z' model). The same effect is seen in the 'Q' model. The difference from the linear ('L') model is small for young peat (Figure 6), but the rate of addition in 'Q' becomes substantially greater than in 'L' in older peat. This results in greater concentrations in peat (Figure 7). The converse is seen for the 'E' model, in which the rate of addition becomes the same at the base as it is in the linear 'L' model, so the rate of addition in 'E' at all earlier ages is always less than in the linear 'L' model, and concentrations are, therefore, substantially smaller than in the other three models.

The percentage of added gas mass that escaped (notionally) to the air in these four simulations was 'Z' 93, 'L' 95, 'Q' 95 and 'E' 96. Given millennia, then diffusion is capable of removing most of the mass of gas generated by decay. In general, the *shape* of the concentration profile does not depend much on the decay model. The exact *position* of the profile is affected by the decay model, but one could not infer the underlying linear, negative exponential, or any other model, from the position alone. We need an independent method for determining how the rate of decay changes down a peat profile.

ACKNOWLEDGEMENTS

MMRW solved the diffusion equations; RSC initiated the work, created the examples, and wrote the first draft of the article.

REFERENCES

Belyea, L.R. (1996) Separating the effects of litter quality and microenvironment on decomposition rates in a patterned peatland. *Oikos*, 77, 529–539.

Clymo, R.S. & Bryant, C.B. (2008) Diffusion and mass flow of dissolved carbon dioxide, methane, and dissolved organic carbon in a 7-m deep raised peat bog. *Geochimica et Cosmochimica Acta*, 72, 2048–2066.

Clymo, R.S. & Pearce, D.M.E. (1995) Methane and carbon dioxide production in, transport through, and efflux from a peatland. *Philosophical Transactions of the Royal Society of London, Series A*, 350, 249–259.

Clymo, R.S., Turunen, J. & Tolonen, K. (1998) Carbon accumulation in peat. *Oikos*, 81, 368–388.

Grant, R.F. & Roulet, N.T. (2002) Methane efflux from Boreal peatlands: theory and testing of the ecosystem model ECOSYS with chamber and tower flux measurements. *Global Biogeochemical Cycles*, 16(4), doi:10.1029/2001GB001702, 2002, 16 pp..

Ingram, H.A.P. (1978) Soil layers in mires: function and terminology. *Journal of Soil Science*, 29, 224–227.

Jähne, B., Heinz, G. & Dietrich, W. (1987) Measurement of the diffusion coefficients of sparingly soluble gases in water. *Journal of Geophysical Research*, 92, 10767–10776.

Romanowicz, E.A., Siegel, D.I., Chanton, J.P. & Glaser, P.H. (1995) Temporal variations in dissolved methane deep in the Lake Agassiz peatlands, Minnesota. *Global Biogeochemical Cycles*, 9, 187–212.

Slade, A.L., Cremers, A.E. & Thomas, H. (1966) The obstruction effects in the self-diffusion coefficients of sodium and cesium in agar gels. *Journal of Physical Chemistry*, 70, 2840–2844.

Walter, B.P., Heimann, M., Shannon, R.D. & White, J.R. (1996) A process-based model to derive methane emissions from natural wetlands. *Geophysical Research Letters*, 23, 3732–3734.

Wania, R., Ross, I. & Prentice, I.C. (2010) Implementation and evaluation of a new methane model within a dynamic global vegetation model: LPJ-WHyMe v1.3. *Geoscientific Model Development Discussions*, 3, 1–59.

Zhuang, Q., Melillo, J.M., McGuire, A.D., Kicklighter, D.W., Prinn, R.G., Steudler, P.A., Felzer, B.S. & Hu, S. (2007) Net emissions of CH₄ and CO₂ in Alaska: implications for the region's greenhouse gas budget. *Ecological Applications*, 17, 203–212.

Submitted 01 Feb 2012, revision 06 Jun 2012

Editor: Olivia Bragg

Author for correspondence:

R.S. Clymo, 49 High Street, Robertsbridge TN32, East Sussex, UK. Email: r.clymo@QMUL.ac.uk